

Pion double charge exchange on  $^{\text{nat}}\text{Se}$ 

P. Hui, H. T. Fortune, R. Gilman,\* C. M. Laymon, and J. D. Zumbro<sup>†</sup>  
*University of Pennsylvania, Philadelphia, Pennsylvania 19104*

P. A. Seidl<sup>‡</sup>  
*University of Texas at Austin, Austin, Texas 78712*

J. A. Faucett<sup>†</sup>  
*New Mexico State University, Las Cruces, New Mexico 88003*  
 (Received 31 August 1993)

Pion-induced double charge exchange ( $\pi^+$ ,  $\pi^-$ ) on a target of  $^{\text{nat}}\text{Se}$  has been investigated at a laboratory angle of  $5^\circ$  and incident kinetic energies of 132, 166, and 294 MeV. Cross sections (and limits) have been extracted for the various ground-state transitions. The double isobaric analog state and several other excited states are also observed.

PACS number(s): 25.80.Gn, 24.30.Cz, 27.50.+e

## I. INTRODUCTION

The pion double charge exchange reaction ( $\pi^+$ ,  $\pi^-$ ) on various nuclei has been studied over a large range of incident pion energies and has generated considerable interest [1]. This double charge exchange (DCX) reaction is very useful in studying special nuclear states, such as the double isobaric analog state and the analog of the isovector giant dipole resonance, which are difficult to populate via other probes. However, information is sparse concerning pion DCX leading to the ground states and to other nonanalog states of the residual nuclei in midmass to heavy nuclei. In fact, the only nuclei with  $A > 58$  for which g.s.  $\rightarrow$  g.s. DCX cross sections have been reported are  $^{60,62,64}\text{Ni}$ ,  $^{88}\text{Sr}$ ,  $^{90}\text{Zr}$ ,  $^{118}\text{Sn}$  (all with limited statistics) [2–4],  $^{93}\text{Nb}$  [5], and  $^{128,130}\text{Te}$  [6]. Recently, some reports have appeared of the population of  $T_{<}$  states below the double isobaric analog state (DIAS) in several nuclei, with the suggestion that such states may be quite a general phenomenon [5–8].

We report here on a study of the pion DCX reaction on a target of natural selenium. This experiment was designed primarily to investigate the ground-state cross section for  $^{80}\text{Se}$ , which makes up 49.6% of  $^{\text{nat}}\text{Se}$  [9]. However, the data also contain the DIAS, as well as several additional excited states.

## II. EXPERIMENTAL PROCEDURE

The experiment was performed at the Energetic Pion Channel and Spectrometer (EPICS) of the Clinton P.

Anderson Meson Physics Facility (LAMPF). Details of EPICS for double charge exchange have been published [10, 11] and will not be repeated here. The target consisted of six cells of  $^{\text{nat}}\text{Se}$  powder, in the configuration displayed in Fig. 1(a). The cells were rectangular with nickel walls. With the configuration shown, the end plugs were either outside the beam area, or could be eliminated during data analysis with horizontal and vertical target cuts in software.

The natural selenium in two of the cells, labeled “inner” in Fig. 1(a) and Table I, had an average areal density of  $1.33 \text{ g/cm}^2$ ; the ones in the four outer cells were significantly thicker, with an average areal density of  $2.13 \text{ g/cm}^2$ . The nickel cell walls had an average areal density of  $0.09 \text{ g/cm}^2$ . The purity of the target powder was about 99%, and the relative abundances of various selenium isotopes are listed in Table II.

An  $x$ -target ( $x$  is vertical at EPICS) histogram is displayed in Fig. 1(b). Cuts placed at dashed lines eas-

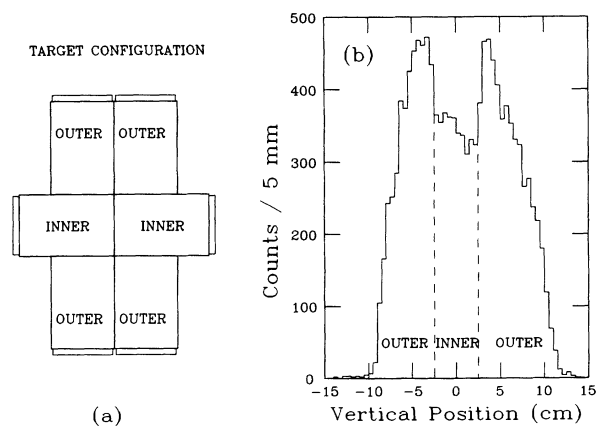


FIG. 1. Configuration of the natural selenium target cells during the experiment is shown in (a). A histogram of ( $\pi^+$ ,  $\pi^-$ ) events vs their vertical positions on the target is shown in (b).

\*Present address: Rutgers, The State University of New Jersey, Piscataway, NJ 08855-0849.

<sup>†</sup>Present address: Los Alamos National Laboratory, Los Alamos, NM 87545.

<sup>‡</sup>Present address: Lawrence Berkeley Laboratory, University of California, Berkeley, CA 94720.

TABLE I. Target information.

Type	Area (cm <sup>2</sup> )	Areal density (g/cm <sup>2</sup> )
<sup>nat</sup> Se (inner cell 1)	38.0	1.32
<sup>nat</sup> Se (inner cell 2)	38.0	1.34
<sup>nat</sup> Se (outer cell 1)	38.4	2.24
<sup>nat</sup> Se (outer cell 2)	38.4	2.13
<sup>nat</sup> Se (outer cell 3)	38.4	2.07
<sup>nat</sup> Se (outer cell 4)	38.4	2.08
CH <sub>2</sub>	229.6	0.07368

ily allowed separation of data into inner and outer cells. Elastic ( $\pi^-$ ,  $\pi^-$ ) scattering was done on the selenium targets, in order to obtain a peak shape to use in the analysis. Straggling and other contributions to the resolution produced full widths at half maxima (FWHM) of 414 keV and 702 keV for inner and outer cells, respectively. Absolute normalizations were obtained from  $\pi$ - $p$  scattering from a CH<sub>2</sub> target of areal density 73.68 mg/cm<sup>2</sup> and comparing the yields with cross sections calculated from  $\pi$ -nucleon phase shifts [12]. The acceptance of the spectrometer was determined from pion inelastic scattering on <sup>12</sup>C at a given angle by varying the spectrometer field to cover an outgoing pion momentum range of about  $\pm 10\%$  of the central momentum of the spectrometer.

Because the momentum acceptance of EPICS is a function of position on the target, the acceptance for the two different <sup>nat</sup>Se targets was slightly different, as displayed in Fig. 2(a). Throughout the analysis, the inner and outer data have been treated independently. The difference in target thickness is sufficient to produce a noticeable difference in resolution, in addition to the different normalizations and energy losses. Hence, even after correcting the spectra for normalization and energy shift, it was not possible to add the two sets of data together and

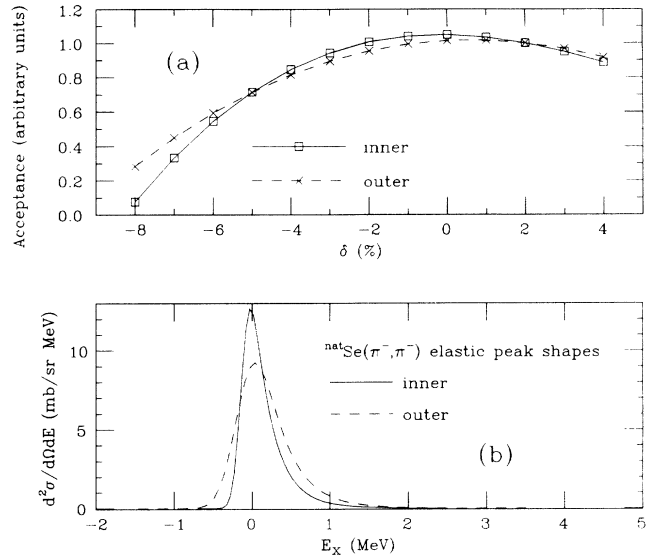


FIG. 2. Relative spectrometer acceptance as a function of  $\delta = \frac{p - p_c}{p_c}$ , where  $p$  is the outgoing pion momentum and  $p_c$  is the central momentum of the spectrometer, is plotted in (a), and <sup>nat</sup>Se( $\pi^-$ ,  $\pi^-$ ) elastic peak shapes at 166 MeV are shown in (b).

treat the sum as a single data set—the peak shapes were just too different [see Fig. 2(b)].

Data were collected at a laboratory angle of 5° and at three incident pion energies: 132, 166, and 294 MeV. Additional shorter runs also exist for  $T_\pi = 102$  and 192 MeV, but they have not been analyzed in the present work.

Individual histograms and their sums at the three energies are displayed in Fig. 3 (not normalized and before acceptance corrections) and in Figs. 4 and 5 (normalized

TABLE II. Differential cross sections of Se( $\pi^+$ ,  $\pi^-$ )Kr(g.s.) at  $\theta_{lab} = 5^\circ$ .

$A_{target}$	Relative abundance <sup>a</sup>	$-Q_{g.s.}$ (MeV) <sup>b</sup>	$T_\pi$ (MeV)	$-Q_{g.s.}$ (MeV) <sup>c</sup>	$\sigma_{g.s.}$ (nb/sr) <sup>d</sup>
76	9.0%	5.27	132		< 207
			166		< 195
			294		< 153
77	7.6%	3.34	132	$3.27 \pm 0.36$	$190 \pm 160$
			166	$3.43 \pm 0.30$	$230 \pm 150$
			294		< 194
78	23.5%	1.86	132	$1.90 \pm 0.27$	$220 \pm 120$
			166	$1.82 \pm 0.22$	$160 \pm 79$
			294		< 74
80	49.6%	-1.15	132	$-1.06 \pm 0.22$	$161 \pm 54$
			166	$-1.11 \pm 0.09$	$70 \pm 23$
			294		< 46
82	9.4%	-4.02	132		< 73
			166	$-4.40 \pm 0.50$	$79 \pm 57$
			294		< 384

<sup>a</sup>From Ref. [9].

<sup>b</sup>Deduced from the values of mass excesses in the literature [24].

<sup>c</sup>Measured in this work.

<sup>d</sup>Assumes that there is no misidentification of an excited state of a heavier isotope. See text for discussion.

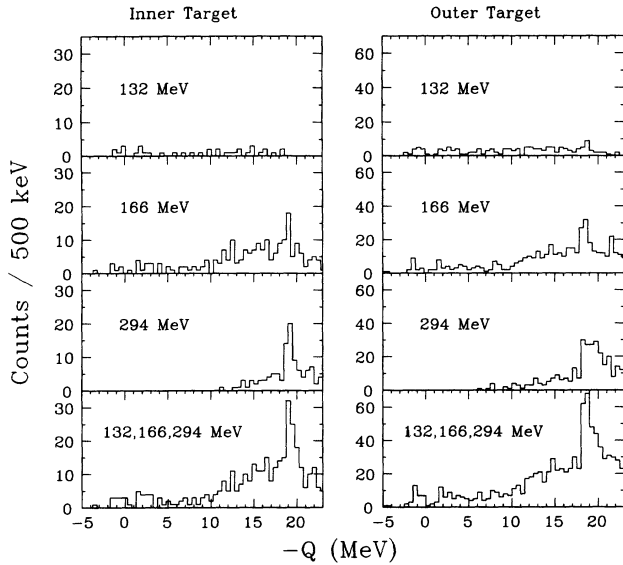


FIG. 3. Spectra of  $^{nat}\text{Se}(\pi^+, \pi^-)\text{Kr}$  at  $5^\circ$  and at three incident pion energies for low  $Q$  values, and the sum of these spectra. The histograms are not normalized and not acceptance corrected.

and acceptance corrected). Several peaks are apparent, and we now turn to their analysis.

### III. ANALYSIS AND RESULTS

Acceptance-corrected histograms were generated and analyzed with the code NEWFIT [13]. For states with no apparent natural width, peak shapes were taken from elastic scattering. For states in the continuum with obvi-

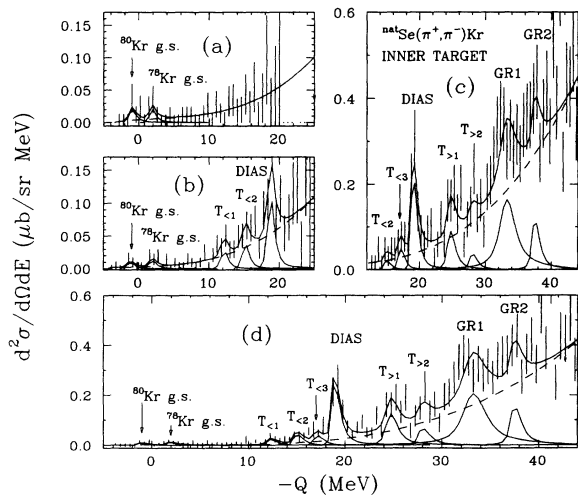


FIG. 4. Inner target spectra of  $^{nat}\text{Se}(\pi^+, \pi^-)\text{Kr}$  at  $5^\circ$  and at the incident pion energy of (a) 132 MeV, (b) 166 MeV, and (c) 294 MeV, and (d) the sum of these spectra. The histograms are absolutely normalized and acceptance corrected. The error bars are statistical only.

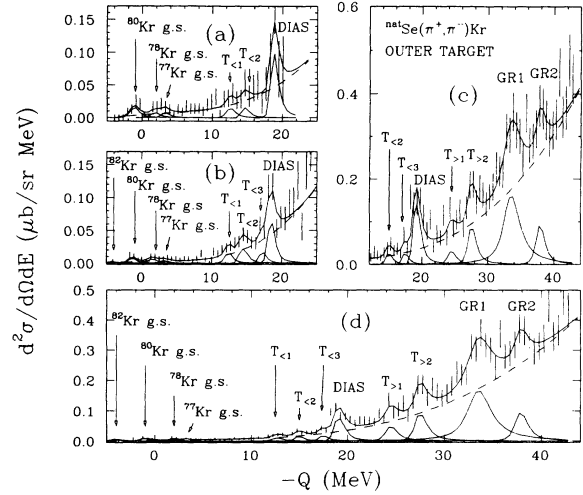


FIG. 5. Outer target spectra of  $^{nat}\text{Se}(\pi^+, \pi^-)\text{Kr}$  at  $5^\circ$  and at the incident pion energy of (a) 132 MeV, (b) 166 MeV, and (c) 294 MeV, and (d) the sum of these spectra. The histograms are absolutely normalized and acceptance corrected. The error bars are statistical only. Note that the  $T_{<3}$  peak is unresolved from the DIAS at 132 MeV.

ous width, this shape was convoluted with a Lorentzian. Following standard practice in analyzing pion DCX data, the background was assumed to be described by a third-order polynomial in  $Q$  [14, 15]. Peaks at low excitation were analyzed as described above, and also by putting area gates on the peaks of interest and simply summing the counts. Background at these low excitations is quite low, but it has been subtracted.

At 132 and 166 MeV, the peak corresponding to  $^{80}\text{Kr}$  (g.s.) is obvious, and those results have already been included in a global survey [4]. Excess counts exist at locations corresponding to some of the other Kr (g.s.), and they have been analyzed accordingly. Of course, as  $Q$  values increase with  $A$ , it is always possible that an excited state from one Se isotope could masquerade as the g.s. from a lighter one. If these are the ground states we are seeing, their cross sections are given in Table II. At 294 MeV, the g.s. results are only upper limits (mostly too large to be informative). Our results from the two different sections of the target are consistent, in both  $Q$  value and cross section. Certainly for  $^{80}\text{Se}$ , and indeed for the average of the other ground states (or excited states, if that is what they are), the cross sections are larger at 132 MeV than at 166 MeV. In other nonanalog g.s.  $\rightarrow$  g.s. transitions, the cross sections tend to peak near 164 MeV. However, we do note a trend: In reactions with less negative  $Q$  values, the peak is at a lower energy—perhaps suggesting that the peak corresponds roughly to the same  $\pi^-$  energy [4, 16].

At higher excitation, the DIAS peak is apparent at all three energies, but at 132 MeV it is just at the edge of the acceptance. Of course, the DIAS peak contains contributions from several Se isotopes; but the various DIAS  $Q$  values are much closer together than our resolution—hence they all appear as a single peak. The DIAS cross sections are listed in Table III and plotted vs  $T_\pi$  in Fig.

TABLE III. Differential cross sections of  ${}^{\text{nat}}\text{Se}(\pi^+, \pi^-)$  to the excited states of krypton at  $\theta_{\text{lab}} = 5^\circ$ .

States	$T_\pi$ (MeV)	$-Q$ (MeV)	$\frac{d\sigma}{d\Omega}$ (nb/sr)	FWHM (MeV)
$T_{<1}$	132	$12.61 \pm 0.54$	$76 \pm 54$	
	166	$12.43 \pm 0.17$	$85 \pm 24$	
	294		$< 84$	
$T_{<2}$	132	$14.76 \pm 0.74$	$72 \pm 65$	
	166	$14.94 \pm 0.17$	$122 \pm 32$	
	294	$14.84 \pm 0.32$	$148 \pm 56$	
$T_{<3}$	132	unresolved from DIAS		
	166	$17.48 \pm 0.40$	$73 \pm 46$	
	294	$17.07 \pm 0.17$	$196 \pm 69$	
DIAS	132	$18.86 \pm 0.24$	$440 \pm 170$	
	166	$18.72 \pm 0.08$	$333 \pm 60$	
	294	$18.92 \pm 0.07$	$1030 \pm 110$	
$T_{>1}$	294	$24.43 \pm 0.18$	$430 \pm 120$	0.5
$T_{>2}$	294	$27.27 \pm 0.08$	$660 \pm 140$	0.5
GR1	294	$33.17 \pm 0.28$	$2770 \pm 290$	$2.1 \pm 1.5$
GR2	294	$37.60 \pm 0.42$	$810 \pm 220$	0.5

6. The curve in Fig. 6 results from a sequential calculation using the code SHIN [17–20] and normalized to the data. If the Se DIAS cross sections obey the systematic trend of Ref. [4], viz.,  $\sigma \propto (N-Z)(N-Z-1)/A^{3.24}$ , and taking into account the isotopic abundance of  ${}^{80}\text{Se}$ , then the  ${}^{80}\text{Se}$  DIAS cross sections deduced from natural selenium data at 166 and 294 MeV are  $376 \pm 68$  nb/sr and  $1160 \pm 130$  nb/sr respectively. At 294 MeV, the DIAS cross section for  ${}^{80}\text{Se}$  is consistent with the systematics within the present uncertainty.

Perhaps the most interesting feature of the current data is the presence of several additional peaks in the continuum. The largest of these has turned out to be the analog of the isovector giant dipole resonance, about which much has been written [14, 15].

At 294 MeV, four peaks above the DIAS are present in both the inner and outer data. They are labeled  $T_{>1}$ ,

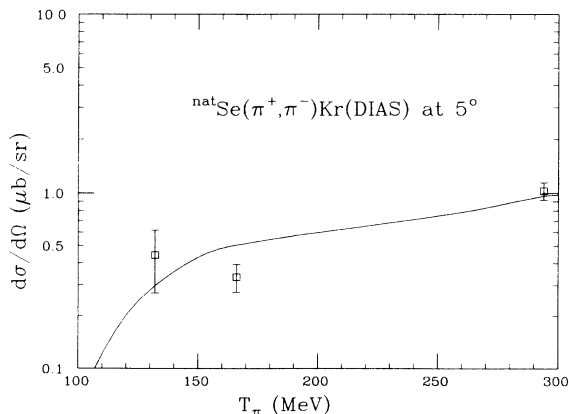


FIG. 6. Forward-angle excitation function of  ${}^{\text{nat}}\text{Se}(\pi^+, \pi^-)\text{Kr}(\text{DIAS})$ . Solid curve results from simple theoretical calculations (see text for explanation).

$T_{>2}$ , GR1, and GR2 in Table III. The GR1 peak (which is the GDR  $\otimes$  IAS) has been fitted with a Lorentzian of 2.1 MeV width folded with the elastic line shape; the other three with  $\Gamma = 0.5$  MeV. The identity of these other three peaks is not known. However, a smaller, narrower peak just above the GDR  $\otimes$  IAS appears to be a general feature in data from other targets [15, 21–23]. In these midmass nuclei, the isospin Clebsch-Gordan coefficients significantly favor the  $T-1$  member of the isospin triplet. It is therefore unlikely that the upper peak is another isospin component of the GDR  $\otimes$  IAS. It could perhaps result from deformation splitting of the underlying dipole resonance. However, because this  $T-1$  giant dipole is totally absent in photonuclear work, where  $T_Z$  restricts the GDR to  $T$  and  $T+1$  members, no information is available concerning its deformation splitting.

Of course, in the present case, this upper peak might be the GDR  $\otimes$  IAS from another Se isotope. That possibility is not very likely for at least three reasons: (1) a width of 0.5 MeV, compared with 2.1 MeV for the lower peak, (2) the strength of 29% relative to GR1 is a bit large, and (3) the energy difference of 4.43 MeV is quite large for an isotopic shift. The biggest argument against this interpretation might be its apparent presence in DCX on monoisotopic targets [15, 21–23]. Clearly, this peak deserves further study.

The two peaks between the DIAS and GR1 have somewhat different strength ratios for the inner and outer parts of the target, but the strengths are consistent within the uncertainties. We have no explanation for these two peaks. We tried (in vain) to assign them to a target impurity. We concluded that they probably arise from DCX on Se. (They might be even more interesting if they did come from a trace impurity in the target, because then their cross sections would be enormous.) We have no way of knowing their isospin—the designation  $T_{>}$  is meant to differentiate them from the  $T_{<}$  peaks below the DIAS.

Below the DIAS, the analysis procedure established the existence of a peak if it was present in the inner or outer data at at least two of the three bombarding energies. Three peaks survived this test: They are labeled  $T_{<1}$ ,  $T_{<2}$ , and  $T_{<3}$  in Table III. The uncertainties on the cross sections are large, but it does appear that  $T_{<2}$  and  $T_{<3}$  have different dependence on incident energy. At 166 MeV their ratio is  $0.60 \pm 0.41$ , while at 294 MeV it is  $1.32 \pm 0.68$ , where the error bars have been added in quadrature. Similar  $T_{<}$  states have now been observed in several nuclei, from  ${}^{56}\text{Fe}$  to  ${}^{138}\text{Ba}$ , with cross sections of 5–20% of  $\sigma_{\text{DIAS}}$ , and separated from the DIAS by only a few MeV [5–8]. At 294 MeV, the current combined  $T_{<}$  cross section is about 42% of the DIAS value. The two  $T_{>}$  states combined have about the same strength as the DIAS.

#### IV. SUMMARY

Double charge exchange on a target of  ${}^{\text{nat}}\text{Se}$  at three pion energies has provided cross sections (or limits) for the various ground states, and has populated at least

three states below the DIAS and four above it (one of which is the GDR  $\otimes$  IAS). Further study is necessary before the identity of the  $T_{<}$  states and other states above the DIAS can be established.

## ACKNOWLEDGMENTS

We acknowledge financial support from the National Science Foundation and the Department of Energy.

- 
- [1] *Proceedings of the Second LAMPF International Workshop on Pion-Nucleus Double Charge Exchange*, Los Alamos, New Mexico, 1989, edited by W. R. Gibbs and M. J. Letich (World Scientific, Singapore, 1990).
  - [2] D. R. Benton, H. T. Fortune, J. M. O'Donnell, R. Crittenden, M. McKinzie, E. Insko, R. Ivie, D. A. Smith, and J. D. Silk, *Phys. Rev. C* **47**, 140 (1993).
  - [3] K. K. Seth, M. Kaletka, D. Barlow, D. Kielczewska, A. Saha, L. Casey, D. Godman, R. Seth, and J. Stuart, *Phys. Lett.* **155B**, 339 (1985).
  - [4] R. Gilman *et al.*, *Phys. Rev. C* **35**, 1334 (1987).
  - [5] M. A. Kagarlis, H. T. Fortune, P. Hui, S. Loe, D. A. Smith, A. L. Williams, and J. Urbina, *Phys. Rev. C* **47**, 1219 (1993).
  - [6] D. A. Smith, H. T. Fortune, G. B. Liu, J. M. O'Donnell, M. Burlein, S. Mordechai, and A. R. Fazely, *Phys. Rev. C* **46**, 477 (1992).
  - [7] P. A. Seidl *et al.*, *Phys. Rev. C* **42**, 1929 (1990).
  - [8] J. M. O'Donnell, H. T. Fortune, J. D. Silk, S. Mordechai, C. L. Morris, J. D. Zumbro, S. H. Yoo, and C. F. Moore, *Phys. Rev. C* **46** 2259 (1992).
  - [9] *CRC Handbook of Chemistry and Physics*, first student ed. (CRC Press, Boca Raton, Florida, 1988), B-128.
  - [10] S. J. Greene, Ph.D. thesis, University of Texas at Austin, Los Alamos National Laboratory Report No. LA-8891-T, 1981.
  - [11] S. J. Greene *et al.*, *Phys. Rev. C* **25**, 927 (1982).
  - [12] G. Rowe, M. Salomon, and R. H. Landau, *Phys. Rev. C* **18**, 584 (1978).
  - [13] C. L. Morris, computer code NEWFIT (unpublished).
  - [14] S. Mordechai *et al.*, *Phys. Rev. Lett.* **60**, 408 (1988).
  - [15] S. Mordechai *et al.*, *Phys. Rev. C* **40**, 850 (1989).
  - [16] H. T. Fortune, S. Mordechai, R. Gilman, K. Dhuga, J. D. Zumbro, G. R. Bureson, J. A. Faucett, C. L. Morris, P. A. Seidl, and C. F. Moore, *Phys. Rev. C* **35**, 1151 (1987).
  - [17] R. Gilman, computer code SHIN (unpublished). See the following three references for the theories related to this code.
  - [18] R. Gilman, Ph.D. thesis, University of Pennsylvania, Los Alamos National Laboratory Report No. LA-10524-T, 1985.
  - [19] R. Gilman, H. T. Fortune, M. B. Johnson, E. R. Siciliano, H. Toki, A. Wirzba, and B. A. Brown, *Phys. Rev. C* **34**, 1895 (1986).
  - [20] A. Wirzba, H. Toki, E. R. Siciliano, M. B. Johnson, and R. Gilman, *Phys. Rev. C* **40**, 2745 (1989).
  - [21] S. Mordechai *et al.*, *Phys. Rev. C* **43**, 1111 (1991).
  - [22] Y. Grof *et al.*, *Phys. Rev. C* **47**, 1466 (1993).
  - [23] D. A. Smith *et al.*, *Bull. Am. Phys. Soc.* **38**, 1817 (1993).
  - [24] A. H. Wapstra, G. Audi, and R. Hoekstra, *At. Data Nucl. Data Tables* **39**, 281 (1988).